Title
The afterglow, redshift and extreme energetics of the γ-ray burst of 23 January 1999

Permalink
https://escholarship.org/uc/item/5n4879gj

Journal
Nature, 398(6726)

ISSN
0028-0836

Authors
Kulkarni, SR
Djorgovski, SG
Odewahn, SC
et al.

Publication Date
1999-04-01

DOI
10.1038/18821

Peer reviewed

The afterglow, the redshift, and the extreme energetics of the γ-ray burst 990123

S. R. Kulkarni[1], S. G. Djorgovski[1], S. C. Odewahn[1], J. S. Bloom[1], R. R. Gal[1],
C. D. Koresko[1], F. A. Harrison[1], L. M. Lubin[1], L. Armus[2], R. Sari[3],
G. D. Illingworth[4], D. D. Kelson[5], D. K. Magee[4], P. G. van Dokkum[6],
D. A. Frail[7], J. S. Mulchaey[8], M. A. Malkan[9], I. S. McLean[9], H. I. Teplitz[10],
D. Koerner[11], D. Kirkpatrick[2], N. Kobayashi[12], I. A. Yadigaroglu[13],
J. Halpern[13], T. Piran[13], R. W. Goodrich[14], F. Chaffee[14], M. Feroci[15], E. Costa[15]

[1]Palomar Observatory 105-24, Caltech, Pasadena, CA 91125, USA
[2]Infrared Processing & Analysis Center, Caltech, Pasadena, CA 91125, USA
[3]Theoretical Astrophysics 130-33, Caltech, Pasadena CA 91125, USA
[4]Lick Observatory, Univ. of California, Santa Cruz, CA 95064, USA
[5]Dept. of Terrestrial Magnetism, Carnegie Institution of Washington,
  5241 Broad Branch Rd., NW, Washington DC 20015, USA
[6]Kapteyn Astron. Institute, P.O. Box 800, NL-9700 AV, Groningen, The Netherlands
[7]National Radio Astronomy Observatory, P. O. Box O, Socorro, NM 87801, USA
[8]Observatories of the Carnegie Institution, 813 Santa Barbara Street,
  Pasadena, CA 91101, USA
[9]Dept. of Physics & Astronomy, Univ. of California, Los Angeles, CA 90095-1562, USA
[10]Goddard Space Flight Center, Code 681, Greenbelt, MD 20771, USA
[11]Univ. of Pennsylvania, 4N14 DRL, 209 S. 33rd St., Philadelphia, PA 19104-6396, USA
[12]Subaru Telescope, National Astronomical Observatory of Japan,
  650 N. A'ohoku Place, Hilo, HI 96720, USA
[13]Dept. of Astronomy, Columbia Univ., 538 W. 120th St., New York, NY 10027, USA
[14]W. M. Keck Observatory, 65-1120 Mamalahoa Highway, Kamuela, HI 96743, USA
[15]Istituto di Astrofisica Spaziale, CNR, via Fosso del Cavaliere, Roma I-00133, Italy

Afterglow, or long-lived emission, has now been detected from about a dozen well-positioned gamma-ray bursts. Distance determinations made by measuring optical emission lines from the host galaxy, or absorption lines in the afterglow spectrum, place the burst sources at significant cosmological distances, with redshifts ranging from ∼1–3. The energy required to produce the bright gamma-ray flashes is enormous: up to ∼ 10^{53} erg or 10% of the rest mass energy of a neutron star, if the emission is isotropic. Here we present the discovery of the optical afterglow and the redshift of GRB 990123, the brightest well-localized GRB to date. With our measured redshift of ≥ 1.6, the inferred isotropic energy release exceeds the rest mass of a neutron star thereby challenging current theoretical models for the origin of GRBs. We argue that the optical and IR afterglow measurements reported here may provide the first observational evidence of beaming in a GRB, thereby reducing the required energetics to a level where stellar death models are still tenable.

Almost thirty years after their discovery[1], the distance scale to gamma-ray bursts (GRBs) was finally unambiguously determined just two years ago[2]. Thanks to precise and prompt GRB localizations by the Italian-Dutch satellite, BeppoSAX[3] and the All Sky Monitor[4] aboard the Rossi X-ray Timing Explorer, afterglow emission spanning the wavelength range from X-ray to radio has now been detected in about a dozen events[5,6,7]. This has provided redshift measurements for four bursts: one through the detection of optical absorption lines[2] and three by identifying emission features in the host galaxies[8,9,10]. It is now assumed that a substantial fraction of all GRBs occur at significant cosmological distances ($z \sim$ 1–3).

The large inferred distances imply staggering energetics. In particular, our measured redshift of $z = 3.14$ for GRB 971214 (ref. 8) led us to an inferred isotropic energy loss of 3×10^{53} erg, or $0.1 M_{\odot} c^2$. At that time, this result was seen to challenge most proposed GRB models. The energy estimate can be reduced by invoking non-spherical emitting surface geometry, e.g. jets. However, to date, there is no firm observational evidence for jets in GRBs. Indeed, on statistical grounds, Grindlay[11] and Greiner et al.[12] constrain the "beaming factor" (the reduction in inferred energy release relative to that for the spherical case) to be less than 0.1.

BeppoSAX ushered in 1999 with the discovery of GRB 990123[13], the brightest GRB seen by BeppoSAX to date. It is in the top 0.3% of all bursts, if ranked by the observed fluence[14]. If the inferred energetics of GRB 971214 strained theoretical models, GRB 990123, with a minimum redshift of 1.6 and an inferred isotropic energy release of $1.9 M_{\odot} c^2$, takes them to the breaking point. In this paper, we present optical and infrared observations of GRB 990123, which both establish the distance to this luminous event, and through the observed break in the decay may provide the first observational evidence yet of beaming in a GRB.

The optical and the infrared afterglow

Much of our information about the parameters of GRB explosions (energy, ambient gas density, dynamics) has been obtained from radio and optical afterglow studies. These returns have motivated observers to carry out long-term multi-wavelength studies of the afterglow.

We initiated an optical and IR follow-up program for GRB 990123 on 23.577 January 1999 UT, 3.7 hr after the event, in response to the BeppoSAX preliminary localization[15]. We used a charge coupled device (CCD) at the Palomar 60-inch telescope to image the field of the BeppoSAX localization. We identified a new source by comparing the first CCD image with an image of the field obtained from the Digital Palomar Observatory Sky Survey II (DPOSS), and concluded that this was the optical afterglow of GRB 990123. We promptly reported the discovery to the GRB Coordinates Network[16] (GCN) and the Central Bureau of Astronomical Telegrams. The optical source lies within the tighter BeppoSAX localization[13] obtained a few hours later (see Figure 1).

Continued observations at Palomar, Keck and other observatories showed that the source exhibited the characteristic fading behavior seen in other GRB optical afterglows. The association of the optical transient (OT) with GRB 990123 is therefore secure. Table 1 summarizes the photometric observations of the OT. Included in the table is a single observation[17] obtained from the Hubble Space Telescope (HST); the analysis of the HST data are reported elsewhere[18]. Figure 2 shows the OT light curve in various bands (primarily Gunn r and K) using the photometric data shown in Table 1.

A considerable body of literature[19,20,21,22] has been developed to explain the afterglow phenomenon. Briefly, afterglow can be understood as arising from synchrotron emission from particles shocked by the explosive debris sweeping up ambient medium. Assuming that the electrons behind the shock are accelerated to a power-law differential energy distribution with index $-p$, the simplest afterglow model (e.g. ref. 23) predicts that the afterglow flux, $f_\nu(t) \propto t^\alpha \nu^\beta$ where $f_\nu(t)$ is the flux at frequency ν and t is the time measured with respect to the epoch of the GRB. Interpretation of the afterglow data in the framework of these models can, in principle, yield many interesting parameters of the GRB explosion (e.g. ref. 24,25).

As the OT faded, the K band image of January 28 showed that the host galaxy was only a fraction of an arcsecond displaced with respect to the OT. A proper analysis of the decay of the OT thus requires that we correctly assess the contribution of the host galaxy to the flux of the OT. The adopted values are $K_{\text{host}} = 0.9 \pm 0.3 \, \mu\text{Jy}$ and $r_{\text{host}} = 0.58 \pm 0.04 \, \mu\text{Jy}$; see legend to Figure 2 for additional details. A discussion of the host galaxy can be found in Bloom et al.[18].

In Figure 2 we present the light curve of the OT after subtracting the contribution from the host galaxy and correcting for Galactic extinction. No single power law can fit the r-band curve. We fit two power laws with a break at epoch t_{break} (see Figure 2). The best fit parameters are $\alpha_{1r} = -1.10 \pm 0.03$, $t_{\text{break}} = 2.04 \pm 0.46$ d and $\alpha_{2r} = -1.65 \pm 0.06$. In contrast, the K band data are well fitted by a single power law, $\alpha_K = -1.10 \pm 0.11$. We now discuss the behaviour of the afterglow in the first few days.

The value of α_{1r} and α_K are similar to those measured in other afterglows (e.g. refs. 26,27,8). In the 2–10 keV band the afterglow was observed by a variety of instruments

aboard BeppoSAX starting 6 hr after the burst[13]. From the analysis of these data, $\alpha_X = -1.44 \pm 0.07$. In the framework of the afterglow models, the power law decay index $\alpha = 3(1-p)/4$ or $\alpha = (2-3p)/4$, depending on whether the electrons are cooling on a timescale that is slower or faster than the age of the shock. A value of $p = 2.44$ is consistent with α_{1r}, α_K and α_X; this would require that the X-ray emitting electrons are in the fast cooling regime whereas the electrons emitting photons in the r and the K bands are in the slow cooling regime.

As briefly summarized above, afterglow models predict that the spectrum of the OT should also be a power law and with the spectral index β having a specific relation to α. After correcting for Galactic extinction, one day after the burst we find that $\beta_{rK} = -0.8 \pm 0.1$. This value is what is expected when the electrons emitting optical and IR photons are in the slow cooling regime. In contrast, comparing the X-ray flux six hours after the burst[13] with the interpolated r-band flux (from Figure 2) we find $\beta_{rX} = -0.54$. Such a large value for β is inconsistent with the simple afterglow model. (Supporting this flat spectrum is the observation that the B-band fluxes, although limited, are comparable to the r-band fluxes; see Figure 2.) Selective extinction by intervening dust in the host galaxy is an unlikely explanation given the strong detection of the afterglow in the B band (Table 1) and in the U band[28].

We draw attention to the fact that such a discrepancy between X-ray and optical fluxes is not uncommon and, in our opinion, a similiar discrepancy exists for GRB 971214 and GRB 980703 as well. This topic is worthy of further study since it is indicative of a fundamental violation of at least one basic assumption of the simple afterglow model (spherical geometry, impulsive energy release and only one dominant emission mechanism – synchrotron emission) Indeed, later in this article, we show that the later behaviour of the afterglow is also not consistent with the simplest afterglow model.

Determining the redshift

We obtained spectra of the optical transient source with the Low Resolution Imaging Spectrograph[29] on the Keck II telescope on the night of January 23, 1999. These observations consisted of three spectra, each of about 600-s duration. A quick analysis showed absorption features, indicating that the OT must be at or beyond a redshift of 1.61. A subsequent detailed data reduction yielded the spectrum displayed in Figure 3.

The OT spectrum is marked by prominent absorption lines whose suggested identifications are listed in Table 2, and marked in Figure 3. Similar lines are routinely seen in quasar spectra, and are thought to arise from absorption in intergalactic clouds. Accepting the identifications, we note that all the absorption features can be attributed to a single intergalactic cloud at a redshift $z_{abs} = 1.6004 \pm 0.0008$. The uncertainty in the redshift has approximately equal contributions from random and systematic errors. The absorption is relatively strong, suggesting the absorbing system has a high column density of gas. This is only the second time that an absorption redshift has been determined for a GRB OT (the other case being GRB 970508 [ref. 2], and possibly also GRB 980703 [ref. 9]), thus placing the OT unambiguously at a cosmological distance.

Although the redshift, $z_{abs} = 1.6$, is a lower limit, it seems likely that the absorption originates in the GRB host galaxy. From the absence of the Lyα forest in our spectrum, we can place a firm upper limit to the redshift of $z < 2.9$. The absence of the reported Lyα forest in the spectrum[30] obtained from the Nordic Optical Telescope (NOT)[30] would further lower this limit to $z \lesssim 2.2$. These limits are further supported by the relatively strong continuum detections of the OT in the B band (see Table 1) and in the U band[28], which suggest little or no absorption by the intergalactic gas.

No other convincing absorption features (aside from the normal telluric absorption) are detected in our spectrum in the wavelength range $\lambda \sim 4700 - 9000$ Å. There are no obvious strong emission lines out to $\lambda \sim 9600$ Å. The absence of other absorption systems in the OT spectrum is not surprising: in this redshift range there is about one metallic line absorber per unit redshift interval[31].

Our slit also included the bright galaxy ~ 10 arcsecond to the West of the OT. We determine a redshift of $z = 0.2783 \pm 0.0005$ for this galaxy, in agreement with the NOT measurement[32]. From our IR observations we note that the K band magnitude of this galaxy is $K = 16.39 \pm 0.03$. At this redshift, this corresponds to a normal, $L \sim L_*$ galaxy.

The energetics of the burst

The combination of a high fluence and a redshift, $z \geq 1.6$, imply that this burst is extremely energetic. For this discussion, we assume a standard Friedmann model cosmology with $H_0 = 65$ km s^{-1} Mpc^{-1}, $\Omega_0 = 0.2$, and $\Lambda_0 = 0$ (if $\Lambda_0 > 0$ then the inferred distance would increase, further aggravating the energetics of the burst). At the redshift $z = 1.6004$, the derived luminosity distance is $D_L = 3.7 \times 10^{28}$ cm, corresponding to the distance modulus $(m - M) = 45.39$, and 1 arcsec in projection corresponds to 8.6 proper kpc, or 22.5 comoving kpc.

From the observed fluence[14] (energy > 20 keV) of 5.1×10^{-4} erg cm^{-2} and the inferred D_L, we estimate the γ-ray energy release, assuming the emission was isotropic, to be 3.4×10^{54} erg $\approx 1.9 M_\odot c^2$, more than the rest mass energy of a neutron star. The prompt optical flash detected by ROTSE[33] had a V magnitude of 8.9, implying a peak luminosity in the UV band (restframe) of $\sim 3.3 \times 10^{16} L_\odot$. This is about a million times the luminosity of a normal galaxy, and about a thousand times the luminosity of the brightest quasars known! The prompt optical emission is attributed to emission from the reverse shock[20,34]; in contrast, the late-time afterglow which is the focus of this paper arises from the forward shock.

The above energetics and the peak luminosities are truly staggering. Popular models suggest that GRBs are associated with stellar deaths, and not with quasars (or the nuclei of galaxies). Perhaps the strongest observational evidence in favor of this presumption is that some GRBs are found offset from their host galaxy, and are therefore not positionally consistent with an active nucleus. An isotropic energy release of $1.9 M_\odot c^2$ is, however, essentially incompatible with the popular stellar death models (coalescence of neutron stars and the currently popular model of the death of massive stars). This large energy release is barely consistent with exotic models such as that of baryon decay[35]; in such models essentially the entire rest mass energy of the neutron star is released.

There are two ways to reduce the estimated energy release. The first possibility is that the burst is amplified by gravitational lensing. Indeed, on the basis of early reports[36] of a possible foreground galaxy near the line of sight to the OT, we proposed that GRB 990123 was lensed. This hypothesis received a boost when the NOT team reported[30] possible intervening systems at redshifts of 0.286 and 0.201 which could be potential candidates for lensing. Our own subsequent, deeper imaging observations have failed to confirm any foreground galaxy and, as discussed above, there is little spectroscopic evidence for the 0.286 and 0.201 absorption systems. There is therefore no direct evidence for lensing at this time.

Furthermore, the lensing probability is $\propto A^{-2}$ where A is the amplification provided by the lens. Even with $A \sim 2$, the expected probability for lensing at a redshift of 1.6 is 10^{-3} (ref. 37). This probability is consistent with the observation that roughly 1 in 500 cosmic radio sources, which likely have a similar redshift distribution to GRBs, are lensed. Thus it is not very likely[38] that one out of the 15 bursts observed by BeppoSAX so far would be highly magnified.

We now consider the second possibility: the emitting surface in GRB 990123 is not spherical. Indeed, almost all energetic sources in astrophysics (e.g. quasars and accreting stellar black holes, pulsars) are not spherically emitting sources but display jet-like geometry. Not surprisingly there is an extensive literature on jets in the GRB context (e.g. refs. 39,40,41,42,43) as well as for the afterglow emission[44].

Should the emitting surface be a jet with an opening angle of radius θ_0 then the inferred energy is reduced from the isotropic value by the beaming factor, $f_b \sim \theta_0^2/2$. Here we make the reasonable assumption based on other astrophysical sources that the jet is two sided. Thus if $\theta_0 \sim 0.3$ then $f_b \sim 5 \times 10^{-2}$, and the γ-ray energy released is $\sim 10^{53}$ erg, a value within reach of current models for the origin of GRBs.

As discussed below, a marked steepening of the afterglow emission is the clearest and simplest signature of a jet-like geometry. The three well studied GRBs (970228, 970508, 980703)[26,45,46,47,48,49] exhibit, at late times (epochs longer than few days) a single power law decay and with indicies that are reasonable for spherical expansion, $\alpha \sim -1.2$. (The complicated early time variations seen in afterglows of many GRBs are not relevant to the discussion here.) The radio afterglow of GRB 970508 has been used to argue[50] for beaming in this source but this result is model dependent. It is against this backdrop that we now proceed to see if there is evidence for non-spherical geometry in GRB 990123.

The shape of the burst: beaming?

Our knowledge of the shape of the emitting region in GRBs is limited because, due to relativistic beaming, only a small portion (angular size $\sim \Gamma^{-1}$, where Γ is the Lorentz factor of the bulk motion of the emitting material) is visible to the observer. Thus the observer is unable to distinguish a sphere from a jet as long as $\Gamma > \theta_0^{-1}$. However, as the source continues its radial expansion, Γ will decrease, and when $\Gamma < \theta_0^{-1}$ there will be a marked decrease in the observed flux. Even if the jet continues to evolve as a cone with a constant opening angle, the observer will see the flux reduced by the ratio of the solid

angle of the emitting surface ($\propto \theta_0^2$) to that expected for a spherical expansion ($\propto \gamma^{-2}$). Thus the light curve will steepen by $\gamma^2 \theta_0^2 \propto t^{-3/4}$. This is a purely geometric effect.

Rhoads[51] makes the important point that unless the jet is confined by some mechanism (as advocated in ref. 43) the jet will also expand sideways at the sound speed of shocked relativistic material, $c_s = c/\sqrt{3}$. Thus as the jet evolves, the solid angle of the emitting region increases as $\pi(\theta_0 + c_s t_{\rm co}/ct)^2$, where t is the time since the burst in the GRB frame, and $t_{\rm co} = t/\Gamma$ is the elapsed time in the frame moving with the jet. When Γ falls below θ_0^{-1} the jet spreads in the lateral direction. Consequently, in this regime, Γ decreases exponentially with radius r instead of as a power law. We can therefore take r to be essentially constant during this spreading phase. Since $t_E \approx r/2\Gamma^2 c$, we find $\Gamma \propto t_E^{-1/2}$ during the spreading phase; here, t_E is the elapsed time in the frame of the observer at Earth. With this scaling the typical synchrotron frequency, ν_m, decreases as t_E^{-2} and the flux at this frequency drops as t_E^{-1}. The flux at a fixed frequency above ν_m drops as $F_\nu = F_{\nu,m}(\nu/\nu_m)^{-(p-1)/2} \propto t_E^{-p}$, where $p \sim 2.5$ is the electron energy power-law index. This is more than one power of t steeper than that for a spherical afterglow, $t_E^{-3(p-1)/4} \propto t_E^{-1.1}$.

In contrast to this discussion, we expect another kind of break and that is when the electrons responsible for the photons in the band of interest enter the cooling regime. In this case, α decreases by $1/4$ (e.g. ref. 23). However, unlike the break due to jet geometry (discussed above) this break is not broad-band. Regardless, in both cases, electron cooling or jets, α is expected to evolve over a timescale of $t_{\rm break}$. Thus the expected change in α, $\Delta\alpha \equiv \alpha_1 - \alpha_2$ is $3/4$ (constant θ_0), $1 - \alpha_1/3$ (spreading jet) or $1/4$ (electron cooling) should be considered to be *upper limits;* see also ref. 52.

As can be seen from Figure 2 we do indeed see a break in the r-band flux with $\Delta\alpha_r = 0.55 \pm 0.07$; the 95% confidence interval, taking into account of covariance with the epoch of the break, is 0.4–0.7 (see Figure 2). On statistical grounds, we can rule out $\Delta\alpha = 1/4$. The prediction of $\Delta\alpha = 1/4$ for cooling electron cooling arises from basic synchrotron theory and is therefore a robust prediction. Therefore, we firmly conclude that the observed break is not due to electron cooling.

The measured value of $\Delta\alpha$ support the hypothesis of a jet in GRB 990123. However, the lack of a break in the K-band light curve is an issue of considerable concern. As explained in the legend to Figure 2, a single power-law model provides a good fit to the K-band data. Within statistical errors we can state that the r-band model does not conform to the K-band light curve. Unfortunately, the quality and quantity of the K-band data and the uncertainty in the adopted flux of the host galaxy do not permit us to derive parameters for a broken power law model independent of those derived from the r-band light curve. [Future K-band observations when the OT has essentially disappeared would help us resolve at least the latter uncertainty.]

We cautiously advance the hypothesis that we are seeing evidence for a jet (perhaps with no sideways expansion). If so, $\theta_0 \sim \Gamma(t_{\rm break})^{-1}$ and for typical parameters $\theta_0 \sim 0.2$ in which case $f_b \sim 0.02$. Thus the energy released in γ-rays alone is 6×10^{52} erg. Including the X-ray afterglow[13] raises the total energy release to 10^{53} erg. GRB 990123 was indeed a very energetic GRB. Following the discovery of the afterglow phenomenon[5,6,7], it was thought

that afterglow observations would provide only global parameters of the GRB explosion (e.g. energy released, ambient density), but it now appears that afterglow observations may give us insight into the geometry of the explosion as well.

Table 1. Photometric observations of GRB 990123

Date (UT)	Telescope	Band	Magnitude	Reference/ Observers
Jan 23.577	P60	r	18.65 ± 0.04	SCO
Jan 23.578	P200	B	18.93 ± 0.04	LML, JSM
Jan 23.958	UPSO	r	20.00 ± 0.05	ref. 53
Jan 24.005	UPSO	B	20.16 ± 0.15	ref. 53
Jan 24.18	BAO	r	20.39 ± 0.15^a	ref. 54
Jan 24.194	BAO	B	20.64 ± 0.07	ref. 54
Jan 24.547	WO	r	20.93 ± 0.2^a	ref. 55
Jan 24.636	KI	K	18.29 ± 0.04	Koerner & Kirkpatrick
Jan 24.934	UPSO	r	21.22 ± 0.08^a	ref. 53
Jan 24.978	UPSO	B	22.06 ± 0.20	ref. 53
Jan 25.14	BAO	r	21.37 ± 0.15^a	ref. 54
Jan 25.940	UPSO	r	21.73 ± 0.12^a	ref. 53
Jan 26.154	BAO	r	22.09 ± 0.10^a	ref. 54
Jan 27.652	KI	K	19.73 ± 0.07	MAM, ISM, HIT
Jan 29.677	KI	K	20.40 ± 0.08	G. Neugebauer & LA
Jan 30.52	MDM	r	23.28 ± 0.18^a	JH, IAY
Feb 3.54	MDM	r	23.88 ± 0.24^a	JH, IAY
Feb 6.6	KI	K	20.84 ± 0.13	NK
Feb 7.610	KI	K	21.00 ± 0.09	SRK
Feb 8.6	KI	K	20.83 ± 0.11	SRK
Feb 9.052	HST	r	24.12 ± 0.10	ref. 18
Feb 9.6	KI	K	20.97 ± 0.10	L. Hillenbrand
Feb 10.6	KI	K	21.21 ± 0.11	L. Hillenbrand
Feb 9.654	KII	r	23.91 ± 0.07^a	A. Filippenko
Feb 14.50	MDM	r	24.10 ± 0.10^a	JH, IAY

Notes:

(1) Telescope Acronyms. P60, Palomar 60-inch telescope. P200, Palomar 200-inch Hale telescope. UPSO, U. P. State Observatory 104-cm telescope. BAO, Bologna Astronomical Observatory 1.5-m telescope. WO, Fred L. Whipple Observatory 1.2-m telescope. KI, Keck-I 10-m telescope. MDM, 2.4-m Hiltner Telescope. KII, Keck-II 10-m telescope. HST, Hubble Space Telescope.

(2) Photometric zeropoint. The night of 23 January UT was photometric at Palomar. Absolute zero-points for the Gunn-r and B-band data were obtained using the observations of standard star-fields[56,57,58]. The absolute zero-point for the K-band observations was obtained using Keck-I data from the night of 24 January UT. Each bandpass zero-point was confirmed independently by at least two members of our group. All subsequent imaging by our group were reduced in the standard manner and photometry was propagated using a set of secondary stars in the GRB field. Photometry derived from data taken in the Cousins R-band were recalibrated to Gunn-r; the quoted uncertainties include the

estimated zeropoint and statistical uncertainties. In this table, we include all of our photometric data obtained to date and also data drawn from the literature which we could reliably place in our B, Gunn-r, and K-band system. Magnitudes marked with the superscript a are R_c magnitudes corrected to Gunn r-band using secondary reference stars reported in ref. 59,36.

Table 2. Absorption Lines Detected in the Spectrum of the OT

Line ID	$\lambda_{obs,air}$ (Å)	$\lambda_{rest,vac}$ (Å)	z	$W_{\lambda,obs}$ (Å)	$\pm$ (Å)
Al III 1862	4843.74	1862.78	1.6010	1.23	0.07
Zn II 2026	5267.29	2026.14	1.6004	2.08	0.17
Cr II 2062	5361.77	2062.23	1.6007	1.26	0.10
Zn II 2062	5361.77	2062.66	1.6002	1.26	0.10
Fe II 2260	5877.17	2260.78	1.6003	0.91	0.07
Fe II 2344	6096.14	2344.21	1.6012	3.04	0.28
Fe II 2374	6173.87	2373.73	1.6016	3.07	0.28
Fe II 2382	6195.29	2382.76	1.6008	3.60	0.40
Fe II 2586	6725.75	2586.64	1.6009	2.84	0.37
Fe II 2600	6759.94	2600.18	1.6005	3.48	0.14
Mg II 2796	7269.47	2796.35	1.6003	4.59	0.30
Mg II 2803	7289.49	2803.53	1.6008	4.80	0.52
Mg I 2852	7416.97	2852.97	1.6005	2.87	0.18

Notes:

(1) $W_{\lambda,obs}$ is the observed line equivalent width; for the restframe values, divide by $(1+z)$.

(2) The observed absorption line at 5362 Å is a blend of two lines, Cr II 2062 and Zn II 2062, and thus it appears twice.

Figure 1. Discovery image of the optical counterpart of GRB 990123. (Left) A 4 arcmin × 4 arcmin portion centered on the OT and extracted from the Digital Palomar Observatory Sky Survey II (DPOSS); the DPOSS is the digitized version of the second Palomar Observatory Sky Survey. (Right) A CCD image in the Gunn-r band obtained at the Palomar 60-inch. The new source, the presumed optical afterglow of GRB 990123, is marked. The circle is the 50-arcsecond localization of the X-ray afterglow[13] as obtained from the Narrow Field Instrument aboard BeppoSAX. Absolute astrometry on the Palomar 60-inch discovery image was obtained by comparison of 34 objects near the optical transient with the USNO-A2.0 V2.0 Catalogue[60]. The r.m.s. uncertainties of the astrometry are $0.28''$(R.A.) and $0.26''$(declination). We find the position of the optical transient to be, $\alpha = 15^{\mathrm{h}}25^{\mathrm{m}}30^{\mathrm{s}}.34$, $\delta = +44^{\mathrm{d}}45'59''.11$ (J2000).

Figure 2. Optical and infrared light curves of the transient afterglow of GRB 990123 from 4 hours to 23 days after the burst. The observed magnitudes from Table 1 have been corrected for Galactic extinction and converted to flux (see below).

(*Top*) The light curve of the transient + host galaxy. From ref. 61 we estimate the Galactic extinction in the direction of the optical transient ($l, b = 73.12°, 54.64°$) to be E(B−V) = 0.01597. Thus, assuming the average Galactic extinction curve ($R_V = 3.1$), the extinction measure is $A_B = 0.069$, $A_r = 0.041$, and $A_K = 0.006$ mag.

(*Bottom*) The inferred light curve of the transient. The contribution of the host flux has been subtracted from the Gunn-r and K-band fluxes at each epoch. The adopted host galaxy fluxes are $K = 22.1 \pm 0.3$ magnitude corresponding to $0.9 \pm 0.3\,\mu$Jy and $0.58 \pm 0.04\,\mu$Jy (Gunn r); see below for details. The error bars include photometric error as well as the uncertainties in the estimated host galaxy flux.

 r-band curve. A single power law decay model is inconsistent with the r-band data ($\chi^2_{\min}/d.o.f \simeq 10$). We then fit the r-band points to a broken power law model: $F_\nu = F_*(t/t_{\rm break})^{\alpha_{1r}}$ for $t \leq t_{\rm break}$ and $F_\nu = F_*(t/t_{\rm break})^{\alpha_{2r}}$ for $t \geq t_{\rm break}$; here, t is the time in days since the GRB and $t_{\rm break}$ is epoch of the break. Using a Levenberg-Marquardt χ^2 minimization[62], we find the r-band data are adequately fit by this broken power-law model ($\chi^2 = 12.1$ for 9 d.o.f.) with the following parameters $F_* = 7.0 \pm 1.9\,\mu$Jy, $t_{\rm break} = 2.04 \pm 0.46$ d, $\alpha_{1r} = -1.10 \pm 0.03$, and $\alpha_{2r} = -1.65 \pm 0.06$. The errors quoted are 1-σ confidence intervals for each respective parameter. Our value of α_{1r} agrees very well with the Sagar et al.'s[53] determination ($\alpha = -1.10 \pm 0.06$), based on B and R observations obtained over the first two nights. There is some covariance between α_2 and $t_{\rm break}$ so that the confidence level on a subset of parameters may extend beyond the above quoted errors. For instance, concurrent values of ($t_{\rm break} = 1$ d, $\alpha_{2r} = -1.5$) are allowed at the 2-σ level as are ($t_{\rm break} = 3$ d, $\alpha_{2r} = -1.8$).

 K-band curve. In contrast, the K-band data can be modelled with a single power law index: $\alpha_K = -1.12 \pm 0.11$ ($\chi^2 = 8.8$ for 6 d.o.f.). This is an acceptable fit (probability of 35%). The K-band data cannot be statistically reconciled to the best fit r-band model (i.e. assuming α_{1r}, α_{2r} and $t_{\rm break}$ to be fixed) with χ^2 ranging from 28 to 66 (7 d.o.f), depending on the value assumed for the flux of the host galaxy.

 The flux of the host galaxy was estimated as follows. For the r-band observations, we used the HST/STIS imaging where the host galaxy is clearly resolved and thus the flux of the OT and the host can be measured quite accurately. In ref. 18 we discuss in great detail the tie between Gunn-r photometry and the STIS photometry (done with CLEAR filter which corresponds approximately to the V band) as well as R-band photometry. The photometric ties are robust so that the flux of the host in r band is well determined, $0.58 \pm 0.04\,\mu$Jy.

 We determined the flux of the host galaxy in K-band as follows. We used the deepest exposures with the best seeing images (February 9 and February 10). In these images the OT is clearly resolved from the host galaxy. Sets of pixels dominated by the OT or by the galaxy were masked, and total fluxes with such censored data were evaluated in photometric apertures of varying radii. Total fluxes of the OT+galaxy were also measured in the same apertures using the uncensored data. We also varied the aperture radii, and the

position and the size of the sky measurement annulus. On February 9 (February 10) UT we find the OT contributes 65 (57) percent (±10 percent) of the total OT+galaxy light. The estimated errors of the fractional contributions of the OT to the total light reflect the scatter obtained from variations in the parameters of these image decompositions. In both epochs the fractional contribution of the host implies a flux of the host galaxy is $0.9 \pm 0.3\,\mu$Jy ($K_{\text{host}} = 22.1 \pm 0.3$ mag). As a further test, we fit the K-band light curve assuming the flux is given as the sum of a power-law (OT) plus a constant flux (host galaxy). This fit yields $K_{\text{host}} = 21.55 \pm 0.20$ magnitude, in agreement with the magnitude derived from direct imaging. However, we note that the fit is barely acceptable ($\chi^2 = 11.9$, 5 d.o.f.).

Figure 3. The spectrum of the optical transient of GRB 990123. Prominent absorption features are marked; all of these can be attributed to various absorption lines at a redshift, $z_{abs} = 1.6004$; the two features labeled as "atm" are telluric absorption features (A and B bands) of the Earth's atmosphere.

Three 600-s integrations were taken, though the last one was terminated after 563 s due to the onset of fog; the integrations commenced at UT 15:38, UT 15:49 and UT 16:01, respectively. The last spectrum also suffered from a higher sky background from the brightening dawn sky. The sky conditions appeared to be good during the first two integrations, with seeing about 1 arcsecond. We used the 300 line/mm grating and the resulting wavelength coverage was 4700 Å to 9000 Å with an effective resolution of about 11.6Å, (full width at half maximum). Spectra were taken with the 1.0 arcsecond wide longslit oriented at position angle (PA) 90° (i.e. East-West) and centered on the OT; the slit also included the prominent galaxy that is about 10 arcsecond West of the OT (see Figure 1).

The usual calibration observations were not obtained given the urgency of the observations. The calibration of the wavelength was obtained using a dispersion curve measured with the same grating and slit, but a somewhat different tilt, ten days earlier. Wavelengths of the unblended night sky emission lines were then used to adjust the zero-point of the wavelength solution fit; this procedure also compensated flexure of the instrument between the exposures. An approximate flux calibration was accomplished by using the instrument response curve also measured 10 days earlier; the instrument response is stable enough for this approach. The slit losses due to the seeing and the difference of the actual slit PA from the optimal (parallactic) angle at the time of observations make the net flux calibration and the overall the shape of the spectrum somewhat uncertain. Nonetheless, we note that our spectroscopic flux measurement is in excellent agreement with photometry from interpolation of the r-band light curve. In any case, this is not important for the redshift measurements discussed in the text.
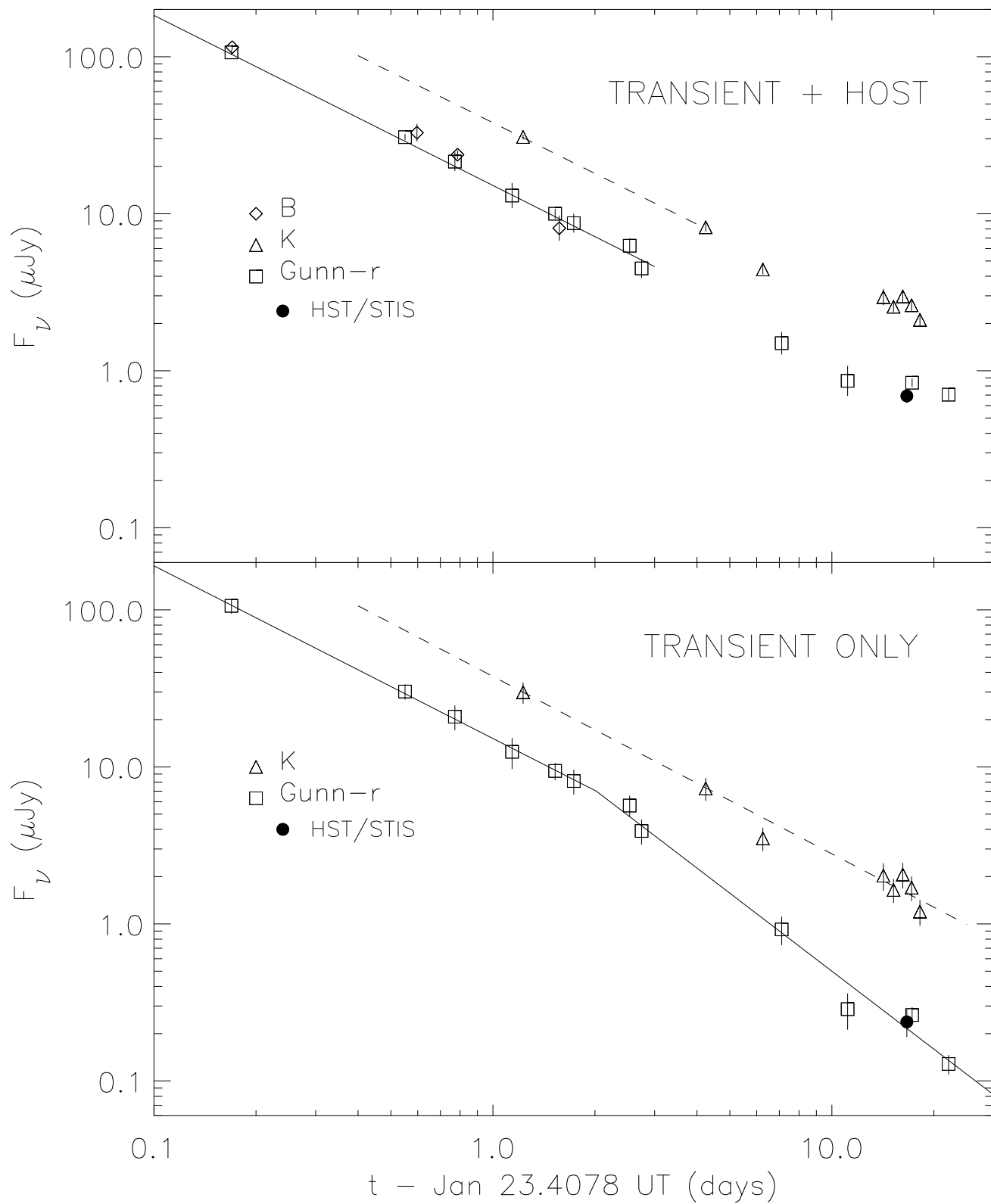
References

1. Klebesadel, R. W., Strong, I. B., & Olson, R. A. Observations of gamma-ray bursts of cosmic origin. *Astrophys. J.* **182**, L85–L88 (1973).

2. Metzger, M. R., Djorgovski, S. G., Kulkarni, S. R., Steidel, C. C., Adelberger, K. L., Frail, D. A., Costa, E. & Frontera, F. Spectral Constraints on the redshift of the optical counterpart to the gamma-ray burst of May 8, 1997. *Nature* **387**, 878–879 (1997).

3. Boella, G. et al. BeppoSAX, the wide band mission for x-ray astronomy. *Astron. Astrophys. Suppl. Ser.* **122**, 299–399 (1997).

4. Levine, A. M., Bradt, H., Cui, W., Jernigan, J. G., Morgan, E. H., Remillard, R., Shirey, R. E. & Smith, D. A. First Results from the All-Sky Monitor on the Rossi X-ray Timing Explorer. *Astrophys. J.* **469**, L33-L36 (1996).

5. Costa, E. et al. Discovery of an X-ray afterglow associated with the gamma-ray burst of 28 February 1997. *Nature* **387**, 783–785 (1997).

6. van Paradijs, J. et al. Transient optical emission from the error box of the γ-ray burst of 28 February 1997. *Nature* **386** 686–689 (1997).

7. Frail, D. A., Kulkarni, S. R., Nicastro, L., Feroci, M. & Taylor, G. B. The radio afterglow from the gamma-ray burst of 8 May 1997. *Nature* **389**, 261–263 (1997).

8. Kulkarni, S. R. et al. Identification of a host galaxy at redshift z=3.42 for the γ-ray burst of 14 Dec 1997. *Nature* **393**, 35–39 (1998).

9. Djorgovski, S. G., Kulkarni, S. R., Bloom, J. S., Goodrich, R., Frail, D. A., Piro, L., & Palazzi, E. Spectroscopy of the Host Galaxy of the Gamma–Ray Burst 980703. Astrophys. J. **508**, L17–L20 (1998).

10. Djorgovski, S. G., Kulkarni, S. R., Bloom, J. S., Frail, D. A., Chaffee, F. & Goodrich, R. GRB 980613: Spectroscopy of the host galaxy. *G.C.N.* **189**, (1999).

11. Grindlay, J. Fast X-ray Transients and Gamma-ray Bursts: Constraints on Beaming. *Astrophys. J.* **510**, 710–714 (1999).

12. Greiner, J., Voges, W., Boller, T. & Hartmann, D. Search for GRB afterglows in the ROSAT all-sky survey. *Astron. Astrophys.,* submitted (1999).

13. Heise, J. et al. A very energetic γ-ray burst on January 23 1999 and its X-ray afterglow. *Nature*, submitted (1999).

14. Kippen, R. M. GRB 990123: BATSE Observations *G.C.N.* **224** (1999)

15. Piro, L. GRB990123, BeppoSAX WFC detection and NFI planned follow-up. *G.C.N.* **199** (1999).

16. The GRB Coordinates Network. http://gcn.gsfc.nasa.gov/gcn/

17. Beckwith, S. For Immediate Posting to GCN – HST Data GRB 990123 Available. *G.C.N.* **254** (1999).

18. Bloom, J. S. et al. The host galaxy of GRB 990123. http://xxx.lanl.gov, astro-ph/9902182 (1999).

19. Katz, J.I. Low-frequency spectra of gamma-ray bursts. *Astrophys. J.* **432**, L110–113 (1994).

20. Mészáros, P., & Rees, M.J. Optical and Long-Wavelength Afterglow from Gamma-Ray Bursts. *Astrophys. J.* **476**, 232–240, (1997).

21. Vietri, M. The Soft X-Ray Afterglow of Gamma-Ray Bursts, A Stringent Test for the Fireball Model. *Astrophys. J.* **478**, L9–12. (1997).

22. Waxman, E. Gamma-ray-burst afterglow: supporting the cosmological fireball model, constraining parameters, and making prediction. *Astrophys. J.* **485**, L5–L8 (1997).

23. Sari, R., Piran, T., Narayan, R. Spectra and Light Curves of Gamma-Ray Burst Afterglows. *Astrophys. J.* **497**, L17–L20 (1998).

24. Wijers, R. A. M. J. & Galama, T. J. Physical parameters of GRB 970508 and GRB 971214 from their afterglow synchrotron emission. http://xxx.lanl.gov, astro-ph/9806175 (1998).

25. Ramaprakash, A. N. et al. The energetic afterglow of the gamma-ray burst of 14 December 1997. *Nature* **393**, 43–46 (1998).

26. Sokolov, V. V., Kopylov, A. I., Zharikov, S. V., Feroci, M., Nicastro, L. & Palazzi, E. BVR$_C$I$_C$ photometry of GRB 970508 optical remnant: May-August 1997. *Astron. Astrophys.* **334**, 117–123 (1998).

27. Groot, P. et al. The decay of optical emission from the gamma-ray burst GRB 970228. *Nature* **387** 479–481 (1997)

28. Falco, E., Petry, C., Impey, C., Koekemoer, A., Rhoads, J. GRB 990123 optical observations. *G.C.N.* **214** (1999).

29. Oke, J. B., Cohen, J. L., Carr, M., Cromer, J., Dingizian, A., Harris, F. H., Labrecque, S., Lucinio, R. Schaal, W., Epps, H. & Miller, J. The Keck Low-Resolution Imaging Spectrometer. *Publ. Astr. Soc. Pacific* **107**, 375-385 (1995).

30. Hjorth, J., Andersen, M. I., Cairos, L. M., Caon, N., Zapatero Osorio, M., Pedersen, H., Lindgren, B., Castro Tirado, A. J. GRB 990123 Spectroscopic Redshifts. *G.C.N.* **219** (1999).

31. Steidel, C. C. & Sargent, W. L. W. Mg II Absorption in the Spectra of 103 QSOs: Implications for the Evolution of Gas in High-Redshift Galaxies. Astroph. J. Suppl. Ser. **80**, 1–108 (1992).

32. Hjorth, J., Andersen, M. I., Pedersen, H., Zapatero-Osorio, M. R., Perez, E., Castro Tirado, A. J. GRB 990123 NOT Spectrum Update. *G.C.N.* **249** (1999).

33. Akerlof, C. W. & MacKay, T. A. GRB 990123. *I.A.U.C.* **7100** (1999).

34. Sari, R. & Piran, T. GRB 990123, The Optical Fash and The Fireball Model. http://xxx.lanl.gov, astro-ph/9902009 (1999).

35. Pen, U.-L. & Loeb, A., Gamma-ray Bursts from Baryon Decay in Neutron Stars. *Astrophys. J.* **509**, 537–543 (1998).

36. Bloom, J. S., Gal, R. R., Lubin, L. L., Mulchaey, J. S., Odewahn, S. C., & Kulkarni S. R. GRB 990123 Optical Follow-up. *G.C.N.* **206** (1999).
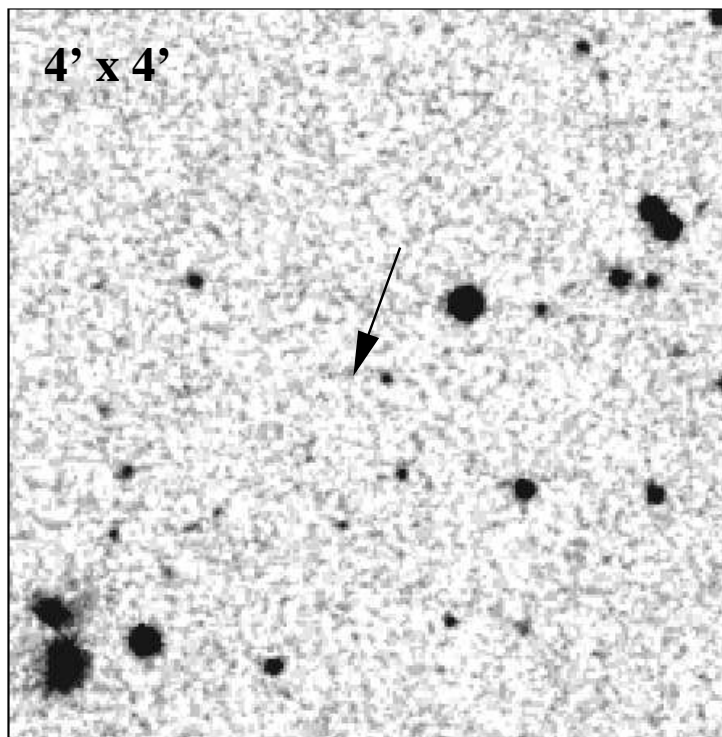
37. Holz, D. E., Coleman, M. M. & Quashnock, J. M. Gravitational Lensing Limits on the Average Redshift of Gamma-ray Bursts. *Astrophys. J.* **510**, 54–63 (1999).

38. Schaefer, B. E. GRB990123, Probability of gravitational lensing. *G.C.N.* **241** (1999).

39. Mochkovich, R., Hernanz, M., Isern, J. & Martin, X. Gamma-ray bursts as collimated jets from neutron star/black hole mergers. *Nature* **361**, 236–237, (1993).

40. Mao, S., & Yi, I. Relativistic beaming and gamma-ray bursts. *Astrophys. J.* **424**, L131–134, (1994).

41. Katz, J. I. Yet Another Model for Gamma Ray Bursts. *Astrophys. J.* **490**, 633–640, (1997).

42. Mészáros, P., & Rees, M.J. Poynting Jets from Black Holes and Cosmological Gamma-Ray Bursts. *Astrophys. J.* **482**, L29–32, (1997).

43. Dar, A. Can Fireball Models Explain Gamma-ray Bursts? *Astrophys. J.* **500**, L93-L96 (1998).

44. Rhoads, J.E. How to Tell a Jet from a Balloon: A Proposed Test for Beaming in Gamma-Ray Bursts. *Astrophys. J.* **478**, L1–L4, (1997).

45. Pedersen, H. et al. Evidence for Diverse Optical Emission from Gamma-Ray Burst Sources. *Astrophys. J.* **496**, 311–315 (1998).

46. Galama, T. et al. Optical Follow up of GRB 970508. *Astrophys. J.* **497**, L13–L16 (1998).

47. Bloom, J. S., Djorgovski, S. G., Kulkarni, S. R. & Frail, D. A. The Host Galaxy of GRB 970508. *Astrophys. J.* **507**, L25–L28 (1998).

48. Fruchter, A. S. et al. The Fading Optical Counterpart of GRB 970228, Six Months and One Year Later. http://xxx.lanl.gov, astro-ph/9807295 (1998).

49. Frail, D. A., Bloom, J. S., Kulkarni, S. R. & Taylor, G. B. The Light Curve and the Spectrum of the Radio Afterglow of GRB 980703. In preparation, (1999).

50. Waxman, E., Kulkarni, S. R. & Frail, D. A. Implications of the Radio Afterglow from the Gamma-Ray Burst of 1997 May 8. *Astrophys. J.* **497**, 288 (1998).

51. Rhoads, J.E. Constraining Gamma Ray Burst Beaming. *Preprint*, (1998).

52. Mészáros, P. & Rees, M. J. GRB 990123: Reverse and Internal Shock Flashes and Late Afterglow Behavior. http://xxx.lanl.gov, astro-ph/9902367 (1999).

53. Sagar, R., Pandey, A. K., Mohan, V., Yadav, R. K. S., Nilakshi, Bhattacharya, D. & Castro-Tirado, A. J. Optical follow up of the GRB 990123 source from UPSO, Nainital. http://xxx.lanl.gov, astro-ph/9902196 (1999).

54. Masetti, N., Palazzi, E., Pian, E., Frontera, F., Bartolini, C., Guarnieri, A., Piccioni, A., & Costa, E. GRB990123, Optical BVRI Observations. *G.C.N.* **233** (1999).

55. Garnavich, P., Jha, S., Stanek, K., Garcia, M. GRB990123, optical observation. *G.C.N.* **215** (1999).

56. Thuan, T. X., & Gunn, J. E. A new four-color intermediate-band photometric system. *Proc. Astron. Soc. Pac.* **88**, 543–547 (1976).

57. Oke, J. B., & Gunn, J. E. Secondary standard stars for absolute spectrophotometry. *Astrophys. J.* **266**, 713–717 (1983).

58. Landolt, A. UBVRI photometric standard stars in the magnitude range 11.5–16.0 around the celestial equator. *Astron. J.* **104**, 340–376 (1992).

59. Zhu, J., & Zhang, H. T. GRB990123 Optical Observation *G.C.N.* **204** (1999).

60. Monet, D. G. The 526,280,881 Objects In The USNO-A2.0 Catalog. *Bull. Amer. Astron. Soc.* **193**, #120.03 (1998).

61. Schlegel, D. J., Finkbeiner, D. P., & Davis, M. Maps of Dust Infrared Emission for Use in Estimation of Reddening and Cosmic Microwave Background Radiation Foregrounds. *Astrophys. J.* **500**, 525–553 (1998).

62. Press, W. H., Teukolsky, S. A., Vetterling, W. T. & Flannery, B. P. *Numerical Recipes in C.* pp 683–699. Cambridge University Press, New York (1992).
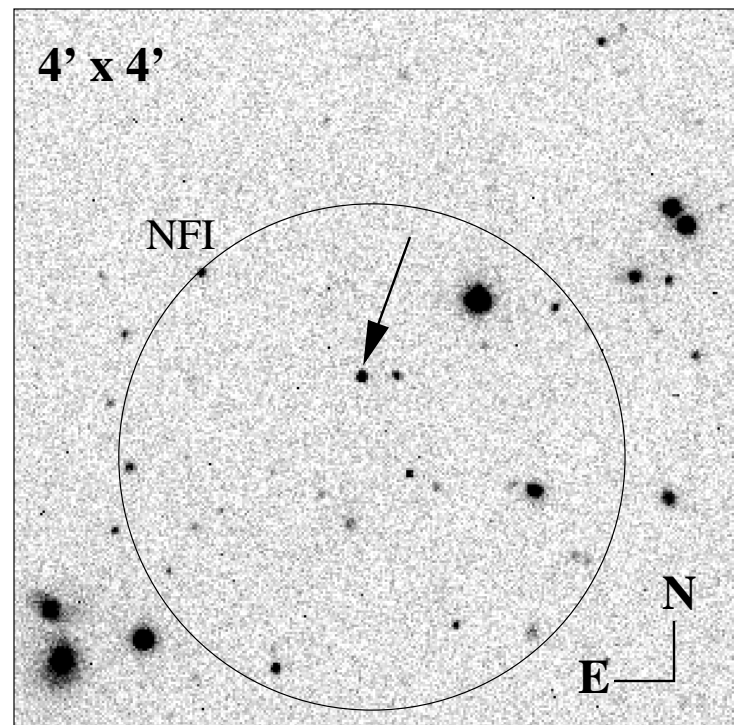
GRB 990123

Palomar 48-inch (DSS)   **Palomar 60-inch**

4' x 4'   4' x 4'

NFI

N
E

July 5 1994 UT   **Jan 23.577 1999 UT**